PIV data and surface view images from analogue experiments on the inheritance of penetrative basement anisotropies by extension-oblique faults

1.   CITATION

This file set contains data reported in the manuscript titled "Inheritance of penetrative basement anisotropies by extension-oblique faults: Insights from analogue experiments." This dataset is freely available under a Creative Commons Attribution 4.0 International (CC-BY 4.0) License. When using the data please cite it as:

Samsu, A., Cruden, A.R., Molnar, N.E., Weinberg, R.F. (2021). PIV data and surface view images from analogue experiments on the inheritance of penetrative basement anisotropies by extension-oblique faults. Monash University. https://doi.org/10.26180/14027243

2.   DATA DESCRIPTION

This dataset includes the results of four analogue experiments on rifting at the Geodynamic Modelling Laboratory of the School of Earth, Atmosphere and Environment at Monash University (Australia). The experiments tested the influence of the width and spacing of penetrative anisotropies in the model ductile lower crust (also referred to as "basement") on fault development in the brittle upper crust (also referred to as "cover") during a single phase of orthogonal extension. Detailed descriptions of the experiments and monitoring by stereoscopic particle imaging velocimetry (PIV) (Adam et al., 2005) can be found in the main text of the manuscript "Inheritance of penetrative basement anisotropies by extension-oblique faults: Insights from analogue experiments", to which this dataset is supplement. An overview of all files included in this dataset is presented in **Samsu_etal_2021_list_of_files.pdf**.

During each experiment, the model was subject to orthogonal extension with an extension velocity of 4.1 cm/hr over a period of 4.5 hrs. An overview of the experiments is presented in Table 1.

Table 1 Overview of experiments. SB = strong basement; NB = normal basement; WZ = weak zones.

Experiment name	Strength contrast between SB & NB	Width/spacing of WZ in SB	Comment
LE-01	low	No WZ	Reference experiment
LE-05	high	No WZ	
LE-07	high	5.4 cm	
LE-08	high	~2 mm	

2.1   Monitoring of experiments

All experiments were monitored using a PIV system comprising three high-speed cameras. Top-view photographs were taken at 16 min intervals. Image pairs recorded at 15 s intervals were used for stereo cross correlation. Quantitative deformation information of the models' surfaces (i.e., strain) was calculated from surface displacements following the workflow of Molnar et al. (2017).

2.2 Data presentation

2.2.1 Top-view videos of surface deformation

Time-lapse videos of deformation at the model surface was compiled from top-view photographs (see Fig. Figure 1 for example) taken at 16 min intervals over a period of four hours. A frame rate of 1 fps was chosen for these image series.
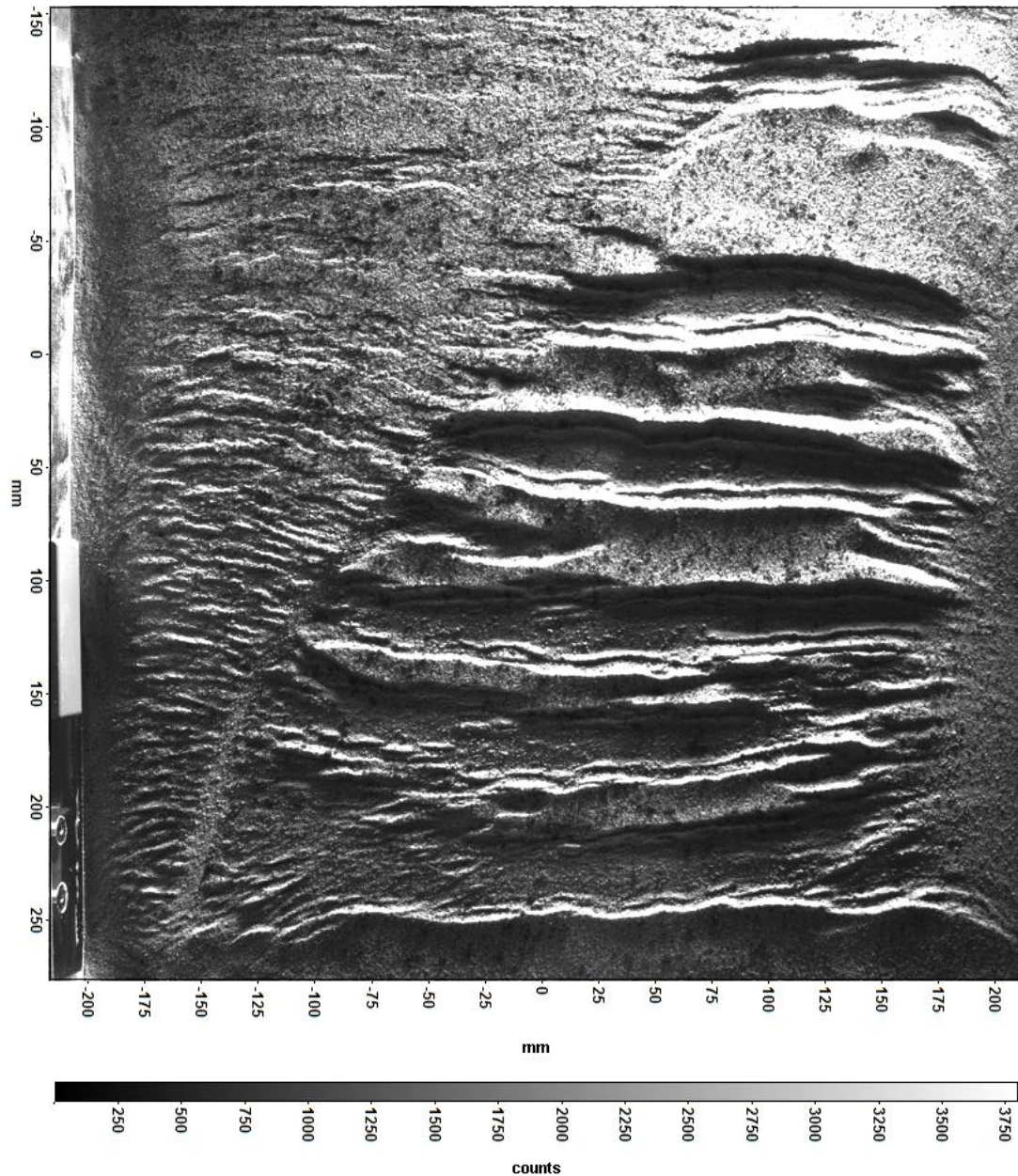

Figure 1 Example of top-view photograph of model surface (Exp LE-05 at end of experiment).

At the end of the experiments, the brittle upper crust material was vacuumed so that the top surface of the ductile lower crust material was exposed (Fig. Figure 2).
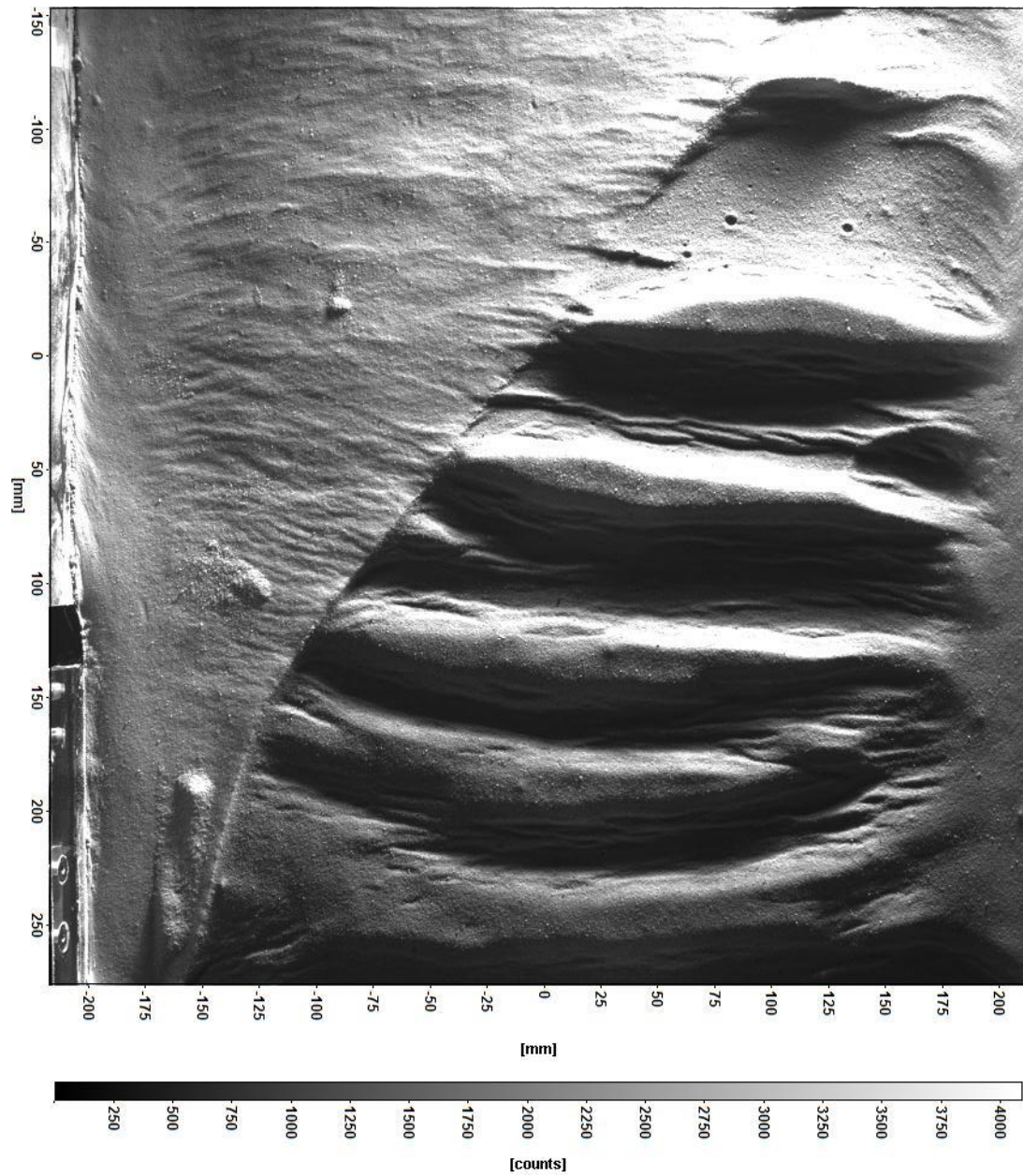

Figure 2 Example of top-view photograph of ductile lower crust (Exp LE-05 at end of experiment).

2.2.3 Evolution of model topography

The change in model topography is presented as time-lapse videos of the model surface height (see Fig. Figure 3 for example). For each experiment, we present an 8 fps video of 102 time steps for Exp LE-05 and 127 time steps for Exp LE-01, LE-07, and LE-08.
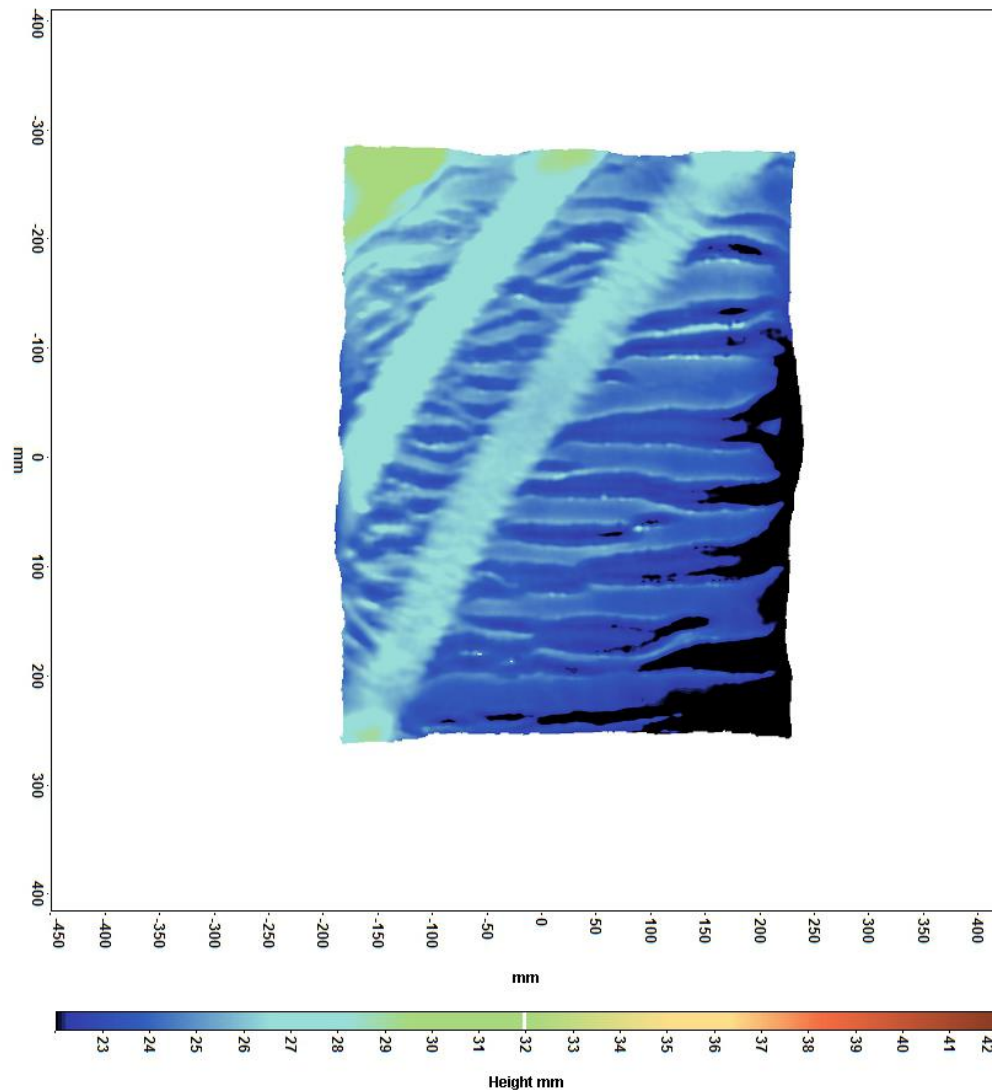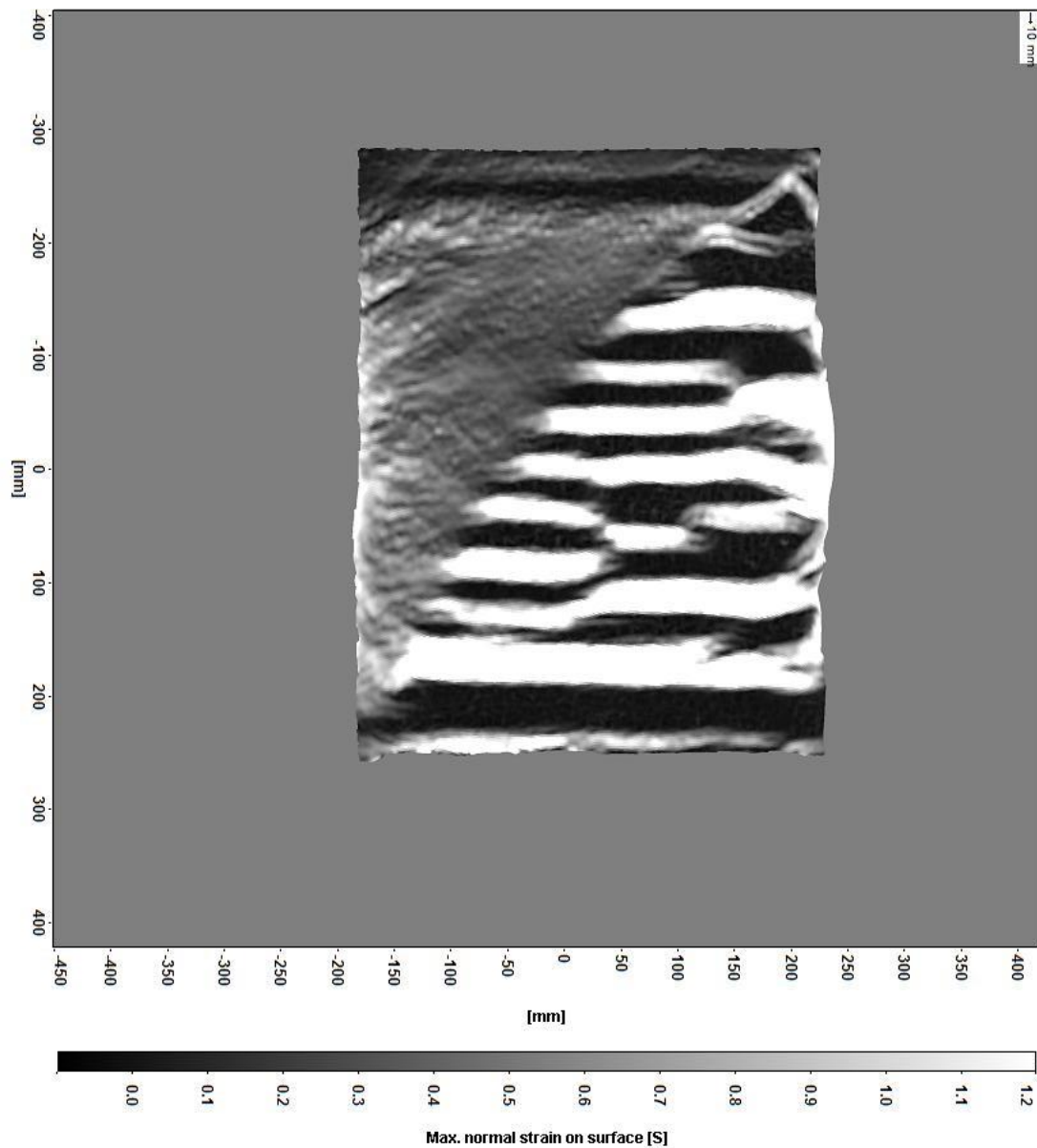

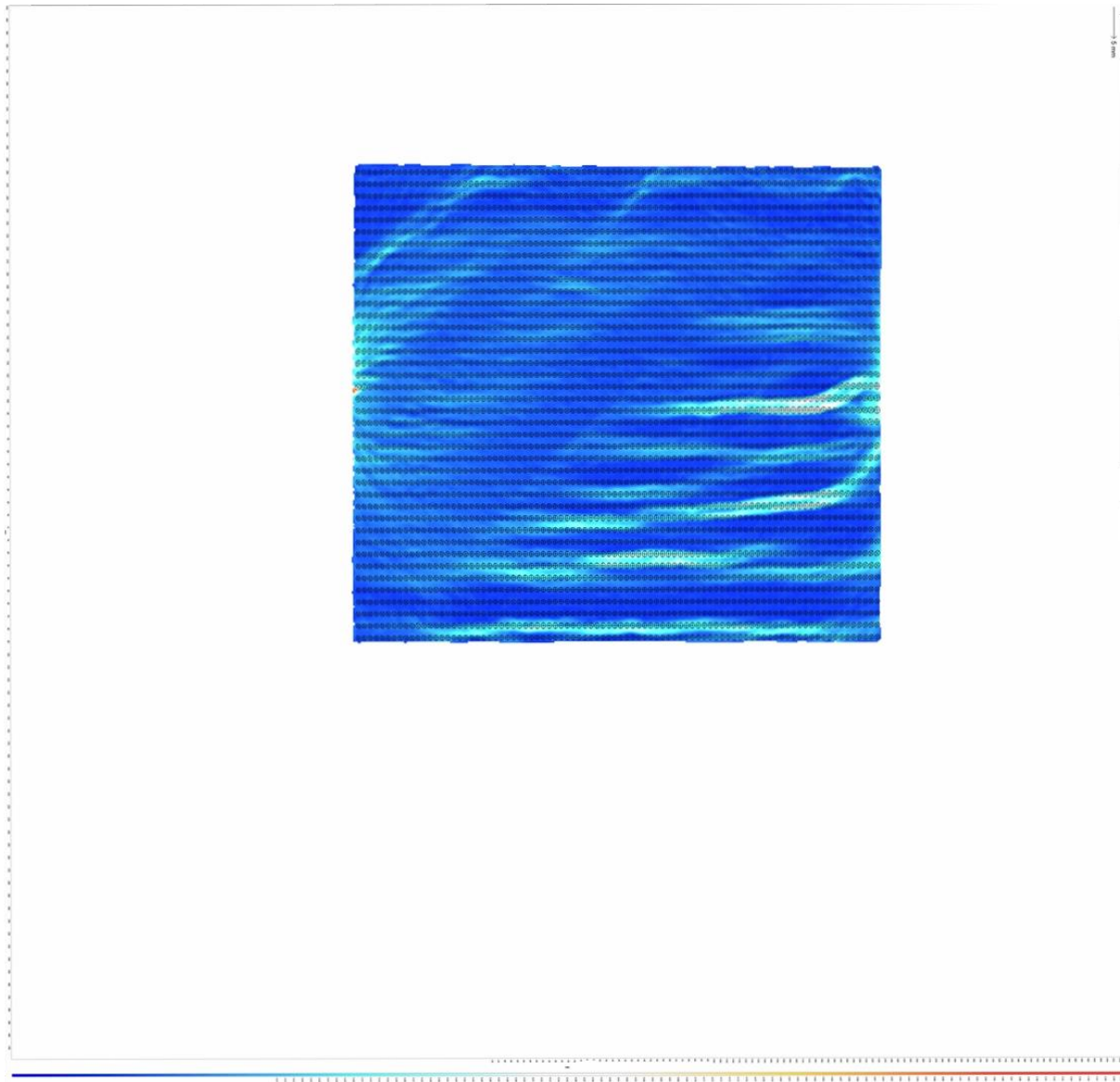**Figure 3 Example of calculated surface height (Exp LE-07 at end of experiment).**

2.2.4   Evolution of cumulative strain

We present four 8 fps videos showing the evolution of the cumulative maximum strain on surface (with 102 time steps for Exp LE-05 and 127 time steps for Exp LE-01, LE-07, and LE-08). We also present another set of two 8 fps videos where strain ellipses are overlain on the cumulative maximum strain on surface (with 127 time steps for both Exp LE-07 and LE-08). Examples are shown in Fig. Figure 4 and Figure 5.

Figure 4 Example of calculated cumulative maximum normal strain on surface (Exp LE-08 at end of experiment).

Figure 5 Example of calculated cumulative maximum normal strain on surface with overlay of strain ellipses (Exp LE-07).

3.   REFERENCES

Adam, J., Urai, J. L., Wieneke, B., Oncken, O., Pfeiffer, K., Kukowski, N., et al. (2005). Shear localisation and strain distribution during tectonic faulting—new insights from granular-flow experiments and high-resolution optical image correlation techniques. *Journal of Structural Geology*, *27*(2), 283–301. https://doi.org/10.1016/j.jsg.2004.08.008

Molnar, N. E., Cruden, A. R., & Betts, P. G. (2017). Interactions between propagating rotational rifts and linear rheological heterogeneities: Insights from three-dimensional laboratory experiments. *Tectonics*, *36*(3), 420–443. https://doi.org/10.1002/2016TC004447